Influence of Cooperative α Dynamics on Local β Relaxation during the Development of the Dynamic Glass Transition in Poly(*n*-alkyl methacrylate)s

F. Garwe, A. Schönhals,† H. Lockwenz, M. Beiner, K. Schröter, and E. Donth*

Universität Halle, Fachbereich Physik, D-06099 Halle (Saale), Germany, and Institut für Angewandte Chemie Berlin-Adlershof, Rudower Chaussee 5, D-12489 Berlin, Germany

Received May 8, 1995; Revised Manuscript Received October 13, 1995[⊗]

ABSTRACT: The development of the dynamic glass transition in poly(*n*-alkyl methacrylate)s is investigated with broad-band dielectric spectroscopy in the frequency range from 10^{-4} to 10^{9} Hz. The experimental data were analyzed by adjustment with one or a sum of two Havriliak Negami functions. Upon decreasing the temperature, the high-temperature relaxation (a) changes into the local β relaxation (Johari Goldstein mode), and the cooperative α relaxation sets in close to this aβ transition. For poly(*n*-butyl methacrylate) a separate onset (zero intensity) of the α process and a parallel course of both traces in the Arrhenius diagram were observed. The activation energy of the β process does not change in spite of the parallel development of the α process. On the other hand, for poly(ethyl methacrylate) the α onset is close to a bend in the local process, i.e., the activation energy of the latter changes after the α onset. In both materials the intensity of the α process linearly increases with falling temperatures but with different intensity. Several scenarios for the αβ-splitting region are suggested.

Introduction

Poly(*n*-alkyl methacrylate)s are an interesting class of materials from several points of view. On the one hand, poly(*n*-alkyl methacrylate) derivatives recently gain an increasing interest as advanced materials for application in nonlinear optics, holographic data handling, and energy storage. An improvement of the relevant material properties needs a better understanding of the molecular dynamics in these polymers, especially an understanding of the undesired back orientation of oriented chromophores for nonlinear optical applications[1,2] and of the influence of the side chain movements on the charge transport in solid state electrolytes based on poly(*n*-alkyl methacrylate)s.[3]

On the other hand, these problems are connected to the dynamics of the glass transition (α process), which is still poorly understood.[4,5] Until now it is not clear what happens in the frequency and temperature range where the one high-temperature process (a or αβ process) splits up into two processes[6] (α or the cooperative process and the local β or Johari Goldstein process[7]). The general interest in such phenomena was induced by the mode-coupling theory describing, for the time being, another splitting, the bifurcation at very high frequencies[8−10] between a cage-rattling process (sometimes called β_{fast}) and the main transition αβ or (a) process.

Poly(*n*-alkyl methacrylate)s are useful materials for studying the splitting because the separation and development of the α process from the αβ process are in a frequency range easily accessible for dielectric and mechanical spectroscopy. A further advantage is that the dielectric intensities of both the α and β processes are relative large and comparable.

There is little doubt that the glass transition is a cooperative phenomenon (for a recent reference, see, e.g., 11), but nearly all the details of what the concept of cooperativity could mean are unknown, e.g., (i) at which temperature and frequency does the cooperative α dynamic set in for a given substance, (ii) how does the conventional local β process separate from the α process (splitting region), and are there different scenarios for this splitting, (iii) does the development of the cooperative α process influence the local β relaxation or not, and (iv) how does the length of the alkyl side chain influence the splitting behavior in the polymers investigated here.

Experimental information about polymer dynamics can be obtained, on the one hand, by relaxational methods (for instance, dynamic shear spectroscopy,[12−14] dielectric spectroscopy,[6,15−21] 2D NMR and 2D magic-angle spinning (MAS) NMR,[22,23] and perhaps heat spectroscopy[24−26]) and, on the other hand, by dynamic scattering experiments (e.g., photon correlation spectroscopy (PCS)[27,28] and, in principle, neutron scattering[29]).

We used broad-band dielectric spectroscopy in a frequency range from $f = 10^{-4}$ to 10^{9} Hz and in a temperature range from −50 to 180 °C to investigate both the β and α relaxations in a large temperature and frequency range around the splitting region. Such a large frequency temperature range is necessary because the splitting regions themselves are rather large and, trying to make a comparison between the different polymers, because the splitting region shifts to lower frequencies and temperatures with increasing side chain length. Preliminary dielectric results for the splitting region of poly(*n*-butyl methacrylate) have been previously published.[30] Some arrays of dynamic shear[13,14] and ^{13}C 2D MAS NMR experiments[23] in the splitting region of poly(*n*-alkyl methacrylate)s were also published.

Experimental Section

Materials. Poly(methyl (PMMA), ethyl (PEMA), *n*-propyl (PnPrMA), and *n*-butyl (PnBMA) methacrylate)s were purchased from Polyscience. Poly(*n*-hexyl methacrylate) (PnHMA) was kindly provided by Dr. G. Meier (Jülich).[31] Table 1 shows several characterization data of the PEMA, PnPrMA, PnBMA, and PnHMA samples. Molecular weights were estimated by gel permeation chromatography with polystyrene

† Institut für Angewandte Chemie Berlin-Adlershof.

[⊗] Abstract published in *Advance ACS Abstracts,* December 1, 1995.

0024-9297/96/2229-0247$12.00/0

Table 1. Characterization of the Samples

sample	M_w (kg/mol)	M_w/M_n	diad syndiotacticity (%)	T_g (DSC) (°C)
PEMA	72.3 ± 3.0	1.9 ± 0.1	78 ± 4	74 ± 1
PnPrMA	bimodal	5.0 ± 0.3	78 ± 4	46 ± 1
	76 ± 5			
	340 ± 20			
PnBMA	330 ± 8	2.35 ± 0.1	78 ± 4	24 ± 2
PnHMA	140 ± 20	2.45 ± 0.2	78 ± 4	0 ± 2

standards. The tacticity of the samples, soluted in nondeuterated THF, was obtained by ^{13}C NMR with a Varian 400 spectrometer. The thermal characterization was performed by a Perkin Elmer differential scanning calorimeter (DSC 7) using heating rates of 10 K/min and sample weights of almost 10 mg. The glass transition temperature is defined as the half-step height temperature. $T_g = 105$ °C was obtained for the conventional PMMA used. Other characterizations on PMMA were not accomplished.

Procedures. Four different equipments were employed for the measurement of the complex dielectric function $\epsilon^*(f) = \epsilon'(f) - i\epsilon''(f)$ (f = frequency, ϵ' = real part, ϵ'' = loss part, i = $\sqrt{-1}$) over 13 decades of frequency. (i) At low frequencies (10^{-4}–10^{-1} Hz) the dielectric measurements are made in the time domain. The density of the depolarization current, $j(t)$, which is related to the time dependent dielectric permittivity by

$$\frac{d\epsilon(t)}{dt} = \frac{j(t)}{E_0\epsilon_0} \quad t > 0 \tag{1}$$

was measured by a Keithley 617 electrometer in a time interval from (0.5 to 5) × 10^4 s after a sample polarization during 3 h with a polarization voltage of 100 V and switching off the electric field E_0 at $t = 0$ (ϵ_0 is the vacuum permittivity). The relation between the experimental $d\epsilon/dt$ data in the time domain and the frequency domain results is given by a Fourier transform. For a first comparison of the data, measured in time and frequency domains, it is convenient to plot the function $(\pi/2)t(d\epsilon(t)/dt)$ over $-\log t - 1$ because this function displays a maximum similar to that of ϵ'' over $\log f$.[32,33] The relation to the frequency scale is given by $ft \approx 0.1$. (ii) A Schlumberger frequency–response analyzer (FRA 1260) supplemented by a buffer amplifier of variable gain[34,35] (10^{-2}–10^6 Hz), (iii) a four-probe HP 4284 A impedance analyzer (10^2–10^6 Hz), and (iv) a coaxial-line reflectometer[35] based on the impedance analyzer HP4191 A (10^6–10^9 Hz) were used.

The samples for the equipments i–iii were pressed between two gold-plated stainless steel electrodes (diameter 20 mm) to a thickness of 250 μm. For the coaxial reflectometer, the capacitor (diameter 5 mm, spacing 50 ± 1 μm) was mounted as a part of the inner conductor of the transmission line.

For the equipments i, ii, and iv, the temperature of the sample was controlled by a custom made nitrogen gas jet heating system covering a broad temperature range from 173 to 493 K with a resolution of ±0.02 K. For the experimental setup (iii), the sample temperature was controlled by a custom made fluid bath cryostat in a temperature range from 273 to 400 K. The absolute temperature deviations between the different equipments were checked to be smaller than 0.5 K. The equilibrating time for each temperature was at least 10 min.

To characterize the relaxation process at a given temperature (T), we used the frequency at maximal loss, $\omega_{max} = 2\pi f_{max}$, the relaxation strength, $\Delta\epsilon$, and shape parameters. The Havriliak Negami (HN) model function[36] was used for the data analysis in both the time and frequency domains. In the frequency domain the HN function reads

$$\epsilon^*(\omega) - \epsilon_\infty = \frac{\Delta\epsilon}{\left(1 + \left(i\frac{\omega}{\omega_0}\right)^b\right)^g} \tag{2}$$

where $f_0 = \omega_0/2\pi$ is the characteristic HN frequency, closely related to (but not identical with) the loss peak frequency, f_{max}, and ϵ_∞ is the real permittivity for high frequencies compared to f_{max}, $\epsilon_\infty \hat{=} \epsilon'(f \gg f_{max})$. The curve shape parameters b and bg ($0 < b < 1$, $0 < bg < 1$) describe the slopes of the ϵ'' curve below and above the frequency of the peak: $b = \partial \log \epsilon''/\partial \log f$ for $f \ll f_0$, and $bg = -\partial \log \epsilon''/\partial \log f$ for $f \gg f_0$. Debye behavior is given by $b = bg = 1$. The conductivity contribution to the dielectric loss is conventionally described by $\epsilon''(\omega) = \sigma/(\epsilon_0\omega)$, where σ is a fitting parameter related to the dc conductivity of the sample. One or a sum of two HN functions (depending on the temperature, see below) was fitted to each isothermal data set using a Gaussian least-squares method.[37]

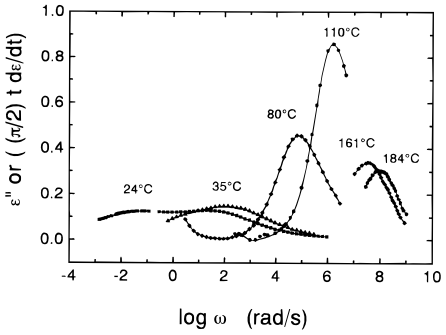

Figure 1. Representative dielectric loss (ϵ'') isotherms for PnBMA. Different frequency regions were measured in different devices (see text). The log symbol always means $\log_{10}$.

The Fourier transform of the HN function for the time domain was numerically calculated according to

$$\frac{d\epsilon_{HN}(t)}{dt} = \int_0^\infty \frac{\Delta\epsilon}{\left(1 + \left(i\frac{\omega}{\omega_0}\right)^b\right)^g} \exp(i\omega t)d\omega \tag{3}$$

and directly fitted to the experimental data. Using this method the data measured in both domains can be analyzed by the same model function. Moreover, a combined evaluation procedure[38] can be used if the determination of the relaxation function requires data from both the frequency and time domains. The frequency of maximal loss (f_{max} for the ϵ'' peak) is calculated from the estimated parameters.

Results

A detailed discussion of the dielectric behavior of the poly(*n*-alkyl methacrylate)s in the $\alpha\beta$-splitting region will be given for PnBMA and PEMA. For the other polymers (PMMA, PnPrMA, and PnHMA) only the loss peak frequencies will be discussed in the Arrhenius diagram.

PnBMA. Figure 1 shows examples of the dielectric loss function for PnBMA in the available frequency range. At high temperatures (e.g., 184 and 161 °C) the intensity of the narrow relaxation curve decreases with increasing temperature. This is possibly the result of the $\langle\mu^2\rangle/kT$ proportionality of $\Delta\epsilon$ ($\langle\mu^2\rangle$ is the mean-square dipole fluctuation, k is Boltzmann constant, and T is temperature). At lower temperatures the intensity gradually decreases (see also Figure 4, below). This unusual behavior of the intensity is discussed below.

For $T > 110$ °C, the relaxation curve is narrow. Figure 1 demonstrates the strong broadening of the ϵ'' curve with decreasing temperature. At 35 °C a shoulder on the low-frequency side of the ϵ'' peak is clearly visible. Two broad but well-separated relaxation processes can be distinguished at 24 °C, the low-frequency one is named by α, the other by β.

Each $\epsilon''(\omega)$ function for $T > 80$ °C can well be fitted by a single HN function without systematic deviations. Figure 2 shows, however, that for temperatures at and

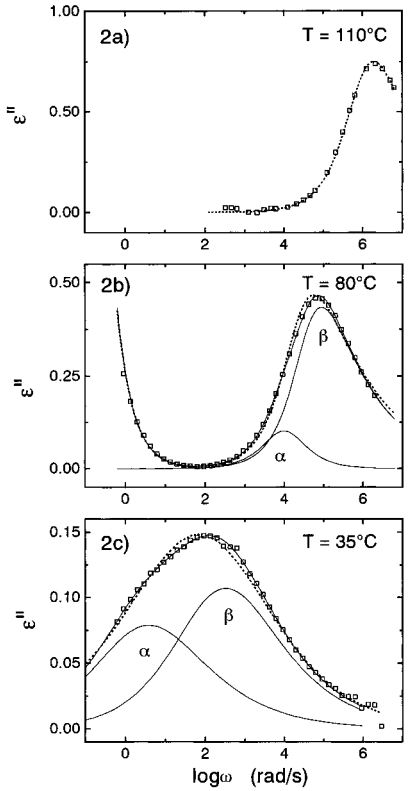

Figure 2. Dielectric loss (ϵ'') as a function of logarithm frequency for PnBMA at three temperatures (110 °C (a), 80 °C (b), 35 °C (c)). The isotherms are fitted with either a single HN function (dotted lines) or an additive superposition of two HN functions (solid lines). The two components of the two-HN fit represent the α and β relaxations. At 80 °C (b) an additional conductivity term was used.

below 80 °C there is a significant difference between a single-HN-function fit (dotted line) and an additive two-HN-function fit (solid line). Detailed analysis using the deviation plot[30] shows a larger and systematic difference for the former. It should be mentioned that the fit algorithm is stable for each isotherm, i.e., different start parameters yield identical final parameters (±10%). The low-frequency HN function represents the cooperative α process, whereas the high-frequency peak represents the local β (Johari Goldstein) process.

The Arrhenius traces (Figure 3 for PnBMA) formally indicate three different regimes (a−c) for the temperature dependence of the maximum frequencies: a high-temperature process (a), the splitting region (b) where the α process is parallel to the β process, and the low-temperature region (c) with the pronounced, curved α process. The adjustment of two HN functions for each temperature ≤ 80 °C gives two stable maximum frequencies for the two fit functions which fit well into two continuous traces although their intensities considerably change with the temperature (Figure 4a). The occurrence of a new phenomenon—the α process—is also indicated by an increase of the β half-width below 80 °C (Figure 4b) and a bend in the ϵ''_{max} curve as a function of temperature (Figure 5). The dynamic shear data for PnBMA[13] also show at first a parallel course of the α and β processes.

In the b regime of the Arrhenius traces in Figure 3, the α and β processes are obviously not independent. This is indicated by the change of the apparent β activation energy in the ab crossover, the change of temperature dependence of $\Delta\epsilon$ intensities, and the

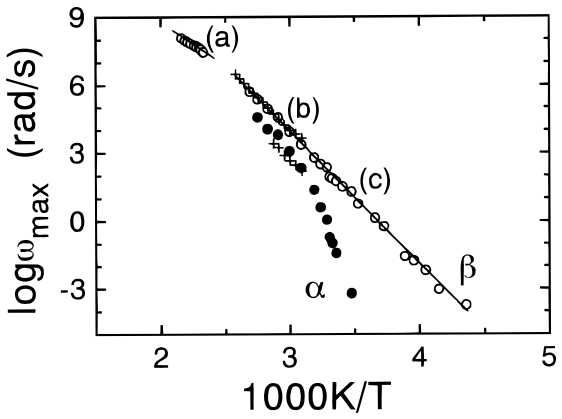

Figure 3. Arrhenius diagram for the $\epsilon''(\omega)$ peak maximum frequencies (ω_{max}) from the HN fits for PnBMA. The α and β traces remain significantly separated and parallel in the splitting region (b regime). Some additional data (+) from device iii (see the Experimental Section) are included to show the independence of the αβ parallelism from the device used. The regimes (a−c) are explained in the text.

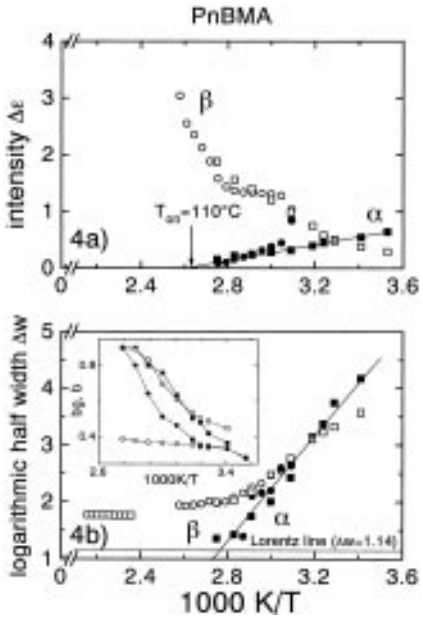

Figure 4. Dielectric intensity ($\Delta\epsilon$) (a) and the full width at half-maximum (Δw) of the ϵ'' peaks (b) as a function of the inverse temperature for PnBMA. The α-onset temperature is obtained from a linear extrapolation to $\Delta\epsilon = 0$; see arrow. The straight line in part b is for the Lorentz line ($\Delta w = 1.144$): (■, ●) α process, (□, ○) β process, (■, □) device ii, and (●, ○) device iii (see the Experimental Section). Insert: HN shape exponents *bg* (●, ○) and *b* (■, □) for the α (●, ■) and β (○, □) processes in PnBMA.

change of the *b* and *bg* shape parameters for the α and β processes (see Figures 3−5).

For lower temperatures, in the c regime of Figure 3, both dielectric traces draw apart. As expected, the α process is now curved similarly to a Vogel Fulcher Tamman (VFT) or Williams Landel Ferry (WLF) law.[39] The slope of the β process trace in the Arrhenius diagram does not change at the bc crossover for PnBMA.

Figure 4 shows the $\Delta\epsilon$ intensities and the values of the full logarithmic width at the half-maximum (Δw) of the ϵ'' peaks for α and β as a function of the temperature. The α intensity linearly increases with decreasing temperature, as expected from a simulation with a modified Fredrickson model.[40] The extrapolation to $\Delta\epsilon = 0$ (α onset) points to a temperature of about 110 °C for PnBMA. In other words, seen from high tem-

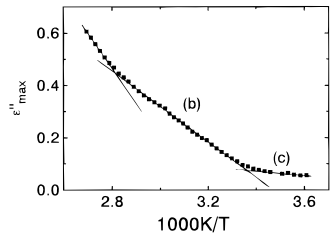

Figure 5. Maximal loss for the different ϵ'' isotherms (without splitting analysis) in the b and c regimes for PnBMA.

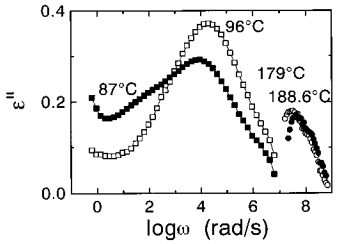

Figure 6. Dielectric loss (ϵ'') as a function of logarithm frequency for PEMA at four temperatures (188.6 °C (●), 179 °C (○), 96 °C (□), 87 °C (■)). The considerable change in the curve shape occurs in the small temperature range 96−87 °C.

perature, the α process starts with zero intensity at 110 °C and log ω (rad/s) = 5.7 and develops with an intensity proportional to the temperature difference (110 °C − T). This is called α onset. The half-width (Δw) of the α process in the b regime remains small (<2 decades). At the α onset it is approximately a Lorentz line, Δw = 1.144. The β intensity decreases with decreasing temperature.

The insert of Figure 4 shows the HN exponents as a function of temperature for both the α and β processes. At high temperatures, both exponents for the α process are large, i.e., the α process is narrow at the onset, as mentioned above. At lower temperatures, both parameters become smaller and have similar values, i.e., the α process becomes broader and retains the symmetrical shape. The β process is asymmetrical (a steeper low-frequency side) at high temperatures and becomes more symmetrical and broader at low temperatures.

PEMA. The change of the dielectric loss function for PEMA is demonstrated in Figure 6. At low temperature the ϵ'' curve becomes broader, and a shoulder can be detected. Unfortunately, below 84 °C the low-frequency flank of the relaxation function is covered by a large conductivity part which makes a reliable adjustment of the α process impossible. Above 96 °C the relaxation curve can be fitted by a single HN function. Figure 7 shows, however, that for temperatures at and below 96 °C a fit with two HN functions is necessary. The low-frequency HN function is assigned to the α process. Figure 8 shows the Arrhenius diagram for PEMA. In contrast to the PnBMA diagram, with its α and β parallelism in the b region, the onset of the α process in PEMA seems to coincide with the bend of the β process in the crossover from the b to the c regime. The latter regime has two processes, α and β, whereas in the b regime for PEMA we only observe the β process but with a larger apparent activation energy than for the a and c regimes.

The intensity of the α process, shown in Figure 9a, again increases linearly with decreasing temperature but is steeper than for PnBMA, whereas the β-process intensity decreases. The α-process onset is at a temperature of 110 °C, just at the bc regime crossover as mentioned above. Both processes have large widths

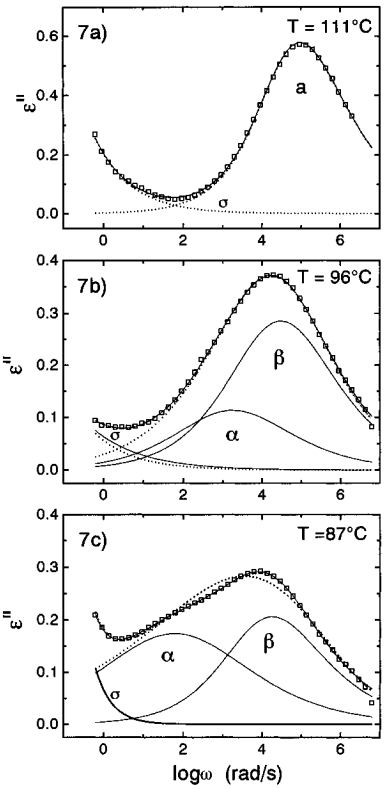

Figure 7. Fit for three ϵ'' isotherms of PEMA with a single HN function (dotted line) and two HN functions (solid line), inclusive conductivity term (σ) in both cases. The two-HN fit is a superposition of an α and β component. The symbols are the experimental data: (a) 111 °C isotherm (only one HN function necessary) and (b and c) 96 and 87 °C isotherms.

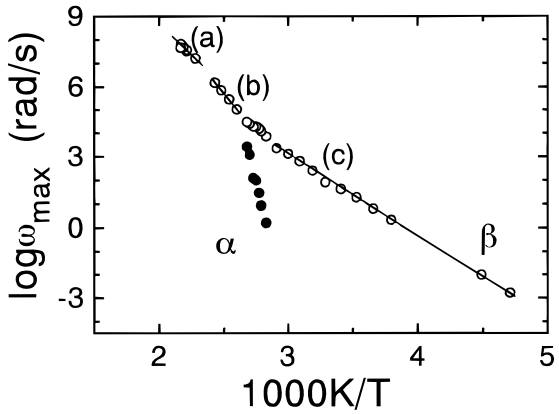

Figure 8. Arrhenius diagram for the position of α (●) and β (○) loss maxima from HN fits for PEMA.

that change slightly with the temperature for PEMA (Figure 9b).

In contrast to PnBMA, the *b* and *bg* HN parameters of the β process (shown in the insert of Figure 9) differ less at high temperatures, i.e., the β process has only a small asymmetry. The *b* and *bg* values become rather similar at lower temperatures. The α process is broad (see Figure 9) and symmetrical ($b \approx bg$).

Other Poly(*n*-alkyl methacrylate)s. A common Arrhenius plot where the PMMA, PnPrMA, and PnHMA data are added is presented in Figure 10. As a general trend the α and β traces, at least for temperatures < 300 K, are at the lower temperatures for the longer side chains (internal plasticification). The bend in the trace of PnHMA indicates that the splitting region for this polymer can be expected near −7 °C and log ω

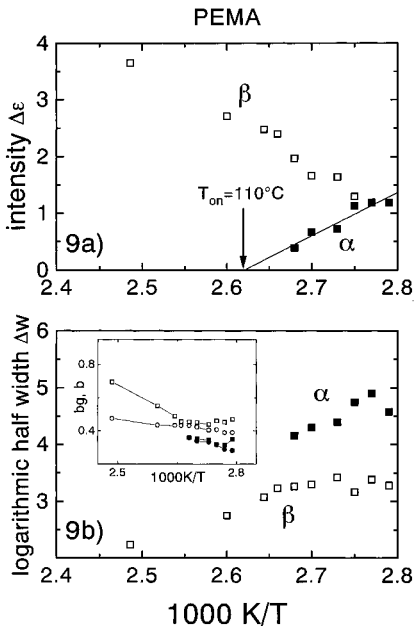

Figure 9. Relaxation strengths ($\Delta\epsilon$) (a) and the full width at half-maximum (Δw) (b) for the α and β components of the HN fits as a function of the temperature for PEMA. The α-onset temperature is determined by a linear extrapolation to $\Delta\epsilon = 0$: (■) α process and (□) β process; all data are taken from device ii. Insert: HN shape exponents *bg* (●, ○) and *b* (■, □) of PEMA for the α (●, ■) and β (○, □) processes.

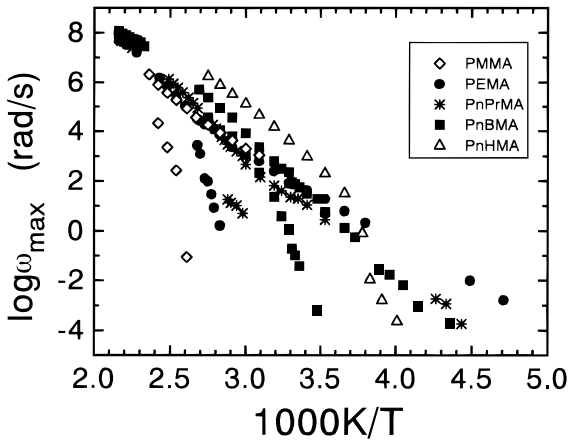

Figure 10. Comparison of ϵ'' peak maxima frequencies (ω_{max}) for the α and β relaxations in PMMA, PEMA, PnPrMA, PnBMA, and PnHMA in a common Arrhenius diagram. PnHMA has a slightly curved trace for $T > 0$ °C.

$= 1$. A more detailed discussion will be given in a future paper.

Discussion

All polymers investigated here have a main dipole moment in the carboxyl group. Both the main chain (polymer backbone) and the side group reorientations can be dielectrically detected, if there is a coupling between them.[12,22]

The increasing intensity ($\Delta\epsilon$ = area below $\epsilon''(\log \omega)$ curve) with falling temperature in the a regime is approximately proportional to $\langle\mu^2\rangle/kT$. The linking of the side groups to the environment is weak. There is sufficient amount of free volume so that the statistical $\langle\mu^2\rangle/kT$ proportionality is operating. In the b regime the intensity decreases with falling temperature (see Figure 1). This can be understood as follows. With falling temperature the interaction to the environment becomes stronger because of the decreasing free volume. The hindered redirection of the carboxyl group operates against the $\langle\mu^2\rangle/kT$ proportionality. Ultimately the possibility for the redirection is very limited because of the small free volume, and an anisotropic dynamics is observed in our polymers above the glass transition temperature.[22]

Table 2. Activation Energies (E_A) and Logarithm of the Limit Frequency (ω_0) Extrapolated to $1/T = 0$ for the Three Regimes (a−c) Defined in Figures 3, 8, and 10[a]

	regime					
	a		b		c	
sample	E_A (kJ/mol)	log ω_0	E_A (kJ/mol)	log ω_0	E_A (kJ/mol)	log ω_0
PMMA			112	19.4	74	14.4
PEMA	109	19.4	128	22.5	65	13.3
PnPrMA	83	16.7	135	22.8	88	13.4
PnBMA	69	15.4	112	21.5	112[b]	21.5[b]

[a] ω_0 is in rad/s. The general uncertainty for E_A is ±5 kJ/mol; for log ω_0, it is ±0.5 decades. [b] PnBMA has no bc crossover in the frequency range observed.

The relaxation rate of the local process in each regime shows an activated temperature dependence according to

$$\ln \omega = \ln \omega_0 - E_A/kT \qquad (4)$$

The activation energies, E_A, and the limit frequencies, ω_0, are determined from the slopes and intersections ($1/T = 0$), respectively, of linear regressions in the Arrhenius diagram for each regime of Figures 3 and 8 separately. Table 2 shows the results for the poly(*n*-alkyl methacrylate)s investigated. In the a regime the activation energy decreases with the side chain length. The ω_0 values are in the range 10^{15}−10^{19} rad/s and seem to be somewhat too large for simple thermal activated processes. A slight curvature of these lines is therefore expected.

The activation energy of the β process in the b regime is larger than the activation energy of the high-temperature process in the a regime for all polymers investigated. The large E_A and high ω_0 values are in conflict with a one-barrier activation. The side chain cannot move alone independently from the neighboring side chains. This points to some coordinated motion of neighboring relaxation units. Therefore the β process in the b regime will be called "locally coordinative". On the contrary, the α process is called "cooperative" and will be connected, after its onset, with increasing number (b regime for PnBMA) and then, after space filling, with increasing size (c regime), and, therefore, decreasing number of the CRR's[30] (CRR = cooperatively rearranging regions, according to Adam and Gibbs).

In the b regime of Figure 10, the β curves for PEMA and PnBMA have similar activation energies but are separated by 1.5 decades in frequency. The polymer with the larger side group (PnBMA) has the *larger* relaxation frequency, when compared to PEMA. This means that we have different kinetic structures of the two locally coordinative processes in the b regime.

The relaxation intensities of both polymers are compared in Figure 11. Although the α-onset temperatures are quite similar (110 °C), the different slopes of intensities clearly reflect differences. The splitting in PEMA is related to a steep onset of the α relaxation. We speculate that the α cooperativity in PEMA is prepared at higher temperatures (b regime) by the locally coordinative β process as a precursor. The trace

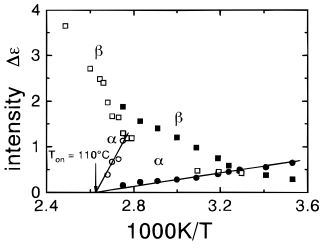

Figure 11. Comparison of dielectric α (●, ○) and β (■, □) relaxation strength for PEMA (○, □) and PnBMA (●, ■).

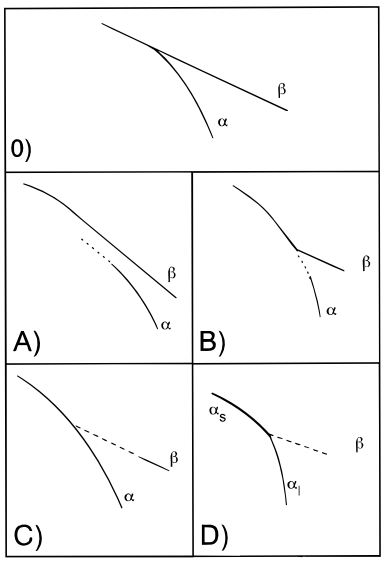

Figure 12. Five general scenarios suggested for the splitting region in the Arrhenius diagram (schematically (—) trace with considerable intensity, (– – –) uncertainty in intensity and trace, (· · ·) intensity tending to zero): (0) conventional, (A) PnBMA type (minimal cooperativity), (B) PEMA type (locally coordinative precursor), (C) PPG type (continuous α transition), and (D) OTP type (crossover between short (α_s) and long (α_l) dynamic glass transition).

of the PEMA α process seems to be curved like a VFT law from the very beginning, whereas the PnBMA α process starts with a straight line parallel to that of the β process. The extrapolated α onset (with zero intensity) for PEMA and PnBMA, however, is nearly at the same position in the common Arrhenius diagram ($T = 110 \pm 5$ °C, log ω (rad/s) $= 5.7 \pm 0.5$).

The β activation energies of poly(*n*-alkyl methacrylate)s in the c regime depend on the side chain length. The activation energy is smaller for shorter side chain lengths, inversely as compared to the a regime. Obviously the local β process is more difficult (higher E_A and lower frequency) for larger side groups in the c regime. This confirms the results obtained in ref 15.

Including the behavior of PnBMA and PEMA, we suggest, as a tentative speculation, five possible scenarios for the $\alpha\beta$-splitting region schematically drawn in Figure 12 (see also refs 30 and 40). The 0 type is sometimes presented in the literature, but, usually, no further details are reported. This type will be called "conventional". A = PnBMA type: This can be described by a modified Fredrickson model[40] where the β process is continuous. The separate α onset can possibly be characterized by a minimal cooperativity for α that cannot be continued to a local, noncooperative process.[41] The dotted lines in Figure 12 always mean that the intensity tends (linearly) to zero near to the last dot. B = PEMA type: There is obviously a locally coordinative β precursor at higher temperatures that prepares the cooperative α process. Below the α-onset temperature, a simpler β process remains (lower c regime E_A value than in the b regime), and the α curvature rests on a cooperativity probably based on combinations of the precursor process. (Remark: Although very improbable from the data analysis, a continuous bending between the a and b regimes for PnBMA and PEMA cannot completely be excluded (see Figures 3 and 8). In the case of a common underlying a−b−α curve, the $\alpha \neq a$ provocation of the A and B type scenarios would be based on the linear increase (from zero) of the α intensity at the onset. A common WLF fit for the a and α traces is not possible with reasonable parameters.) C = PPG (poly(propylene glycol)) type:[42] The "topology" of the diagram is similar to that of the conventional 0 type, but it seems that α is curved above and below the splitting and that β is not the tangent to α. The β intensity, although weak, increases approaching the splitting. The details in the vicinity of the splitting point remain uncertain because of the β weakness (broken line). At the splitting point the character of the α cooperativity seems to change slightly. (The long broken β line means that the intensity cannot be described.) We suggest the development of a thermokinetic[41] structure that allows local β modes only below this point. An exaggerated version of C is the next. D = OTP (*o*-terphenyl) type:[43] Stickel et al.[44] concluded from very precise dielectric experiments, using a new data evaluation method, that there are two different but touching WLF traces in OTP (and some other substances) with a sharp (of about 1 frequency decade) crossover between them and a β trace aiming to this common tangential point, with constant or increasing intensity again. We suggest that this is a crossover between a short (α_s) and a long (α_l) glass transition in the sense of ref 41. The β line can again be understood by the assumption that only the liquid structure organization corresponding to the long transition is capable for a local β process. Generally, at the present stage nothing can be said about the sharpness of the bends or "points" in the scenarios suggested.

Note added at revision: By the way, the name "PnBMA type" for the A scenario is rather limited. Investigating three differently polymerized and prepared "pure" and "similar" PnBMA samples, the A scenario was observed two times (with rather different α-onset temperatures) and the B scenario once. This means that the A scenario is extremely sensitive to molecular details. Moreover, a gradual transition from the A type to the C type scenario was observed in a series of statistical copolymers of a PnBMA with increasing polystyrene contents (S. Kahle et al., to be published). It seems, therefore, that the A scenario in PnBMA is a unique observation.

Conclusions

The evaluation of dielectric broad-band experiments by means of one or a sum of two Havriliak Negami fit function shows that the $\alpha\beta$-splitting behavior in the poly(*n*-alkyl methacrylate)s is much more complex than previously expected. A lot of fine interrelations between α and β and a lot of fine differences between the different polymers are detected. The main results are that the character of the local process can vary considerably in the splitting region (Figure 10), that there are obviously different splitting scenarios (see Figure 12), and that we should expect a succession of slightly different thermokinetic equilibrium structures[41] with

increasing complexity (and characteristic length) when a glass former is cooled.

Acknowledgment. The authors are grateful to the Deutsche Forschungsgemeinschaft for financial support and to Prof. E. W. Fischer and F. Stickel for information about their experimental OTP data prior to publication.

References and Notes

(1) Wang, H.; Jarnagin, C.; Samulski, E. T. *Macromolecules* **1994**, *27*, 4705.
(2) Hoffmann, C. L.; Man, H. T.; Fuller, G. G. *Acta Polym*. **1993**, *44*, 39.
(3) Ohno, H.; Inoue, Y.; Wang, P. *Solid State Ionics* **1993**, *62*, 257.
(4) Creta Conference 1991. *J. Non-Cryst. Solids* **1992**, *131−133*.
(5) Alicante Conference 1994. *J. Non-Cryst. Solids* **1994**, *172−174*.
(6) McCrum, N. G.; Read, B. E.; Williams, G. *Inelastic and Dielectric Effects in Polymeric Solids*; New York, Dover, 1991.
(7) Johari, G. P.; Goldstein, M. *J. Chem. Phys*. **1970**, *53*, 2372. Johari, G. P. *J. Chem. Phys*. **1973**, *58*, 1766; *Ann. N. Y. Acad. Sci*. **1976**, *279*, 117.
(8) Götze, W.; Sjörgren, L. *Rep. Prog. Phys*. **1992**, *55*, 241.
(9) Cummins, H. Z.; Du, W. M.; Fuchs, M.; Götze, W.; Hildebrand, S.; Latz, A.; Li, G.; Tao, N. *J. Phys. Rev*. **1993**, *E47*, 4223.
(10) Bartsch, E.; Fujara, F.; Kiebel, M.; Sillescu, H.; Petry, W. *Ber. Bunsen.-Ges. Phys. Chem*. **1989**, *93*, 1252.
(11) Cicerone, M. T.; Blackburn, F. R.; Ediger, M. T. *J. Chem. Phys*. **1995**, *102*, 471.
(12) Heijboer, J. In *Physics of Noncrystalline Solids*; Prins, J. A., Ed.; North Holland: Amsterdam, 1965; p 231.
(13) Beiner, M.; Garwe, F.; Schröter, K.; Donth, E. *Colloid Polym. Sci*. **1994**, *272*, 1439.
(14) Beiner, M.; Garwe, F.; Schröter, K.; Donth, E. *Polymer* **1994**, *35*, 4127.
(15) Sasabe, H.; Saito, S. *J. Polym. Sci., Part B* **1968**, *6*, 1401.
(16) Ishida, Y.; Yamafuji, K. *Kolloid-Z*. **1961**, *177*, 97.
(17) Williams, G.; Edwards, D. A. *Trans. Faraday Soc. II* **1966**, *62*, 1329. Williams, G. *Trans. Faraday Soc. II* **1966**, *62*, 2091.
(18) Tetsutani, T.; Kakizaki, M.; Hideshima, T. *Polymer J*. **1982**, *14*, 305.
(19) Hofmann, A.; Kremer, F.; Fischer, E. W.; Schönhals, A. In *Disorder Effects on Relaxational Processes*; Richert, R., Blumen, A., Eds.; Springer: Berlin, 1994.
(20) Gomez Ribelles, J. L.; Dias Calleja, R. *J. Polym. Sci., Polym. Phys*. **1985**, *23*, 129.
(21) Floudas, G.; Rizos, A.; Brown, W.; Ngai, K. L. *Macromolecules* **1994**, *27*, 2719.
(22) Kulik, A. S.; Beckham, H. W.; Schmidt-Rohr, K.; Radloff, D.; Pawelzik, U.; Boeffel, C.; Spiess, H. W. *Macromolecules* **1994**, *27*, 4746.
(23) Domberger, W.; Reichert, D.; Garwe, F.; Schneider, H.; Donth, E. *J. Phys.: Condens. Matter* **1995**, *38*, 7419.
(24) Birge, N. O.; Nagel, S. R. *Phys. Rev. Lett*. **1985**, *54*, 2674.
(25) Birge, N. O. *Phys. Rev. B* **1986**, *34*, 1631.
(26) Beiner, M.; Korus, J.; Lockwenz, H.; Schröter, K.; Donth, E. To be published.
(27) Meier, G.; Fytas, G.; Dorfmueller, T. *Macromolecules* **1984**, *17*, 957.
(28) Patterson, G. D.; Jue, P. K.; Ramsay, D. J.; Stevens, J. R. *J. Polym. Sci., Part B* **1994**, *32*, 1137.
(29) Richter, D.; Zorn, R.; Farago, B.; Frick, B.; Fetters, L. J. *Phys. Rev. Lett*. **1992**, *68*, 71.
(30) Garwe, F.; Schönhals, A.; Beiner, M.; Schröter, K.; Donth, E. *J. Phys.: Condens. Matter* **1994**, *6*, 6941.
(31) Giebel, L.; Meier, G.; Fytas, G.; Fischer, E. W. *J. Polym. Sci., Part B* **1992**, *30*, 1291.
(32) Hamon, B. V. *Proc. Instr. Electr. Eng*. **1952**, *151*, 99.
(33) Schönhals, A.; Schlosser, E.; Carius, H.-E. *Acta Polym*. **1990**, *41*, 1991; *42*, 149.
(34) Pugh, J.; Ryan, T. *IEE Conf. Dielectr. Mater. Measurements Applications* **1979**, *177*, 407.
(35) Kremer, F.; Boese, D.; Meier, G.; Fischer, E. W. *Prog. Colloid Polym. Sci*. **1989**, *80*, 129.
(36) Havriliak, S.; Negami, S. *J. Polym. Sci., Part C* **1966**, *14*, 99.
(37) Schlosser, E.; Schönhals, A. *Colloid Polym. Sci*. **1989**, *267*, 963.
(38) Schönhals, A. To be published.
(39) Williams, M. L.; Landel, R. F.; Ferry, J. D. *J. Am. Chem. Soc*. **1955**, *77*, 3701.
(40) Schulz, M.; Donth, E. *J. Non-Cryst. Solids* **1994**, *168*, 186.
(41) Donth, E. *Relaxation and Thermodynamics in Polymers, Glass Transition*; Akademie-Verlag: Berlin, 1992.
(42) Schönhals, A.; Kremer, F. *J. Non-Cryst. Solids* **1994**, *172−174*, 336.
(43) Stickel, F. Dissertation, Universität Mainz, Figure 5.82.
(44) Stickel, F.; Fischer, E. W.; Richert, R. *J. Chem. Phys*. **1995**, *102*, 1.

MA9506142